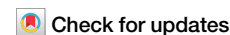


<https://doi.org/10.1038/s41612-024-00771-6>

Recent heatwaves as a prelude to climate extremes in the western Mediterranean region



Ernesto Tejedor¹✉, Gerardo Benito¹, Roberto Serrano-Notivol², Fidel González-Rouco³, Jan Esper^{4,5} & Ulf Büntgen^{5,6,7}

The 2022 and 2023 western Mediterranean summer temperatures exceeded millennial natural variability, reaching unprecedented anomalies of +3.6 °C and +2.9 °C respectively. We show that anthropogenic climate change may turn extreme heatwaves from a rarity of 1 in 10,000 years into events occurring every 4–75 years, depending on future scenarios. This shift underscores the urgency of implementing adaptive strategies as extreme climate events manifest sooner and more intensely than expected.

The Mediterranean basin, home to over 510 million people, has emerged as a focal point for climate change impacts^{1,2}. The summers of 2022 and 2023 exemplified this vulnerability, with the western Mediterranean (WM hereafter) experiencing heatwaves of historic dimensions^{3–5}. The warmth of these events were unprecedented, with temperatures reaching record levels both in the instrumental period and in a millennial-long context (Fig. 1). Despite extensive studies on climate extremes⁵, integrated analyses combining historical reconstructions, instrumental records, and future projections are still lacking for the WM. Here, we aim at enhancing our ability to estimate the frequency of such extremes under different climate scenarios. Our findings underscore an alarming trend: extreme climate phenomena, initially projected to occur towards the end of the 21st century¹, are indeed already occurring, earlier and more fiercely than expected.

While the summer of 2023 was recognized as the warmest in the Northern Hemisphere over the last two millennia⁶, our regional study emphasized 2022, due to its well-documented impacts and greater extremity (Fig. 1). During the May to September warm season of 2022, the WM, including Spain, France, Italy, Morocco and Algeria, experienced temperature anomalies three to four standard deviations above the 1940–2000 climatological mean. Concurrently, sea surface temperatures (SSTs) exceeded instrumental ranges by more than four standard deviations, forming record-breaking marine heatwaves⁵. These extremes were driven by a persistent Azores high, most intense in June and July, which, coupled with minimal cloudiness and intense ground heating, facilitated prolonged heatwaves. This situation propelled Saharan hot air over the WM and much of central Europe³, exacerbating warm synoptic conditions. Record-high sunshine durations, maximum glacier retreats in the European Alps⁵ and

Pyrenees^{7,8}, and severe droughts from low winter and spring precipitation culminated in record low river discharge rates⁵. This, in turn, increased wildfire risks and resulted in the second largest burnt area on record across WM⁵. Such conditions disrupted agricultural water supplies and fueled widespread forest degradation, reducing the summer net terrestrial carbon uptake in the WM region by 56–62 TgC⁹. The human toll was staggering, with over 60,000 heat-related deaths in Europe in the summer of 2022¹⁰, most notably in Italy and Spain. A closer look at Spain's 2022 data reveals record-breaking heat anomalies, making it the warmest summer since 1890 by instrumental records³ and since 1119 CE based on reconstructed data⁴. Likewise, summer 2023 recorded unprecedented high SSTs, especially in the North Atlantic (Fig. 1c, d), causing marine heatwaves across Europe. Southern Europe faced up to 2 weeks of “very strong” heat stress, with “feels-like” temperatures between 38 and 46 °C, and southern Spain experienced up to 60 days of these conditions¹¹.

How rare were the western Mediterranean summer heatwaves of 2022 and 2023?

The 2022 and 2023 warm seasons in the WM were contextualized against instrumental, historical, and projected data. Comparison of probability density functions (PDFs) from past reconstructions and observations reveal a consistent trend, with instrumental data indicating an average increase of 0.2 °C and a significant skew towards more frequent warm extremes at the 95th percentile (Fig. 2a). In order to have the most complete representation of long-term variability and trends in the area we used both EURO-CORDEX¹² (Representative Concentration Pathways, RCPs¹³) and CMIP6¹⁴ (Shared Socioeconomic Pathways, SSPs¹⁵) simulations (Fig. 2a, b).

¹Department of Geology, National Museum of Natural Sciences–Spanish National Research Council (MNCN-CSIC), Madrid, Spain. ²Department of Geography and Regional Planning, Environmental Sciences Institute (IUCA), University of Zaragoza, Zaragoza, Spain. ³Instituto de Geociencias (CSIC-UCM), Consejo Superior de Investigaciones Científicas, Universidad Complutense de Madrid, Madrid, Spain. ⁴Department of Geography, Johannes Gutenberg University, Mainz, Germany. ⁵Global Change Research Institute of the Czech Academy of Sciences, Brno, Czechia. ⁶Department of Geography, University of Cambridge, Cambridge, UK.

⁷Department of Geography, Faculty of Science, Masaryk University, Brno, Czechia. ✉e-mail: Ernesto.tejedor@mncn.csic.es

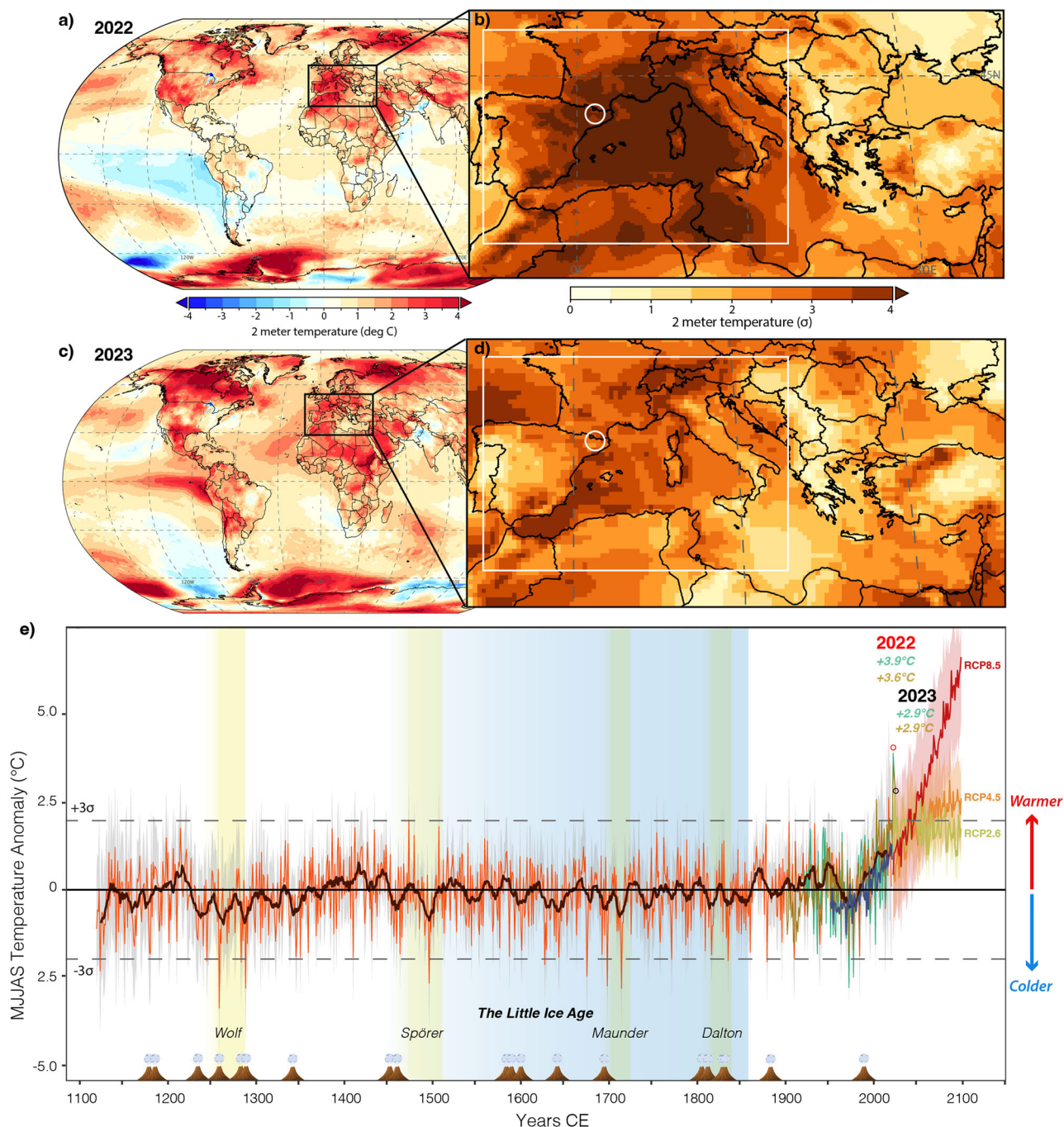


Fig. 1 | Global and regional maximum temperature anomalies for 2023 and 2023: Historical Context and Climate Projections. **a** *Global Perspective:* Temperature anomalies for May through September (MJJAS) 2022, compared against the 1940–2000 baseline, using ERA5 reanalysis data. This global overview highlights the exceptional nature of the 2022 season. **b** *Regional Focus:* Temperature anomalies in 2022 in Southern Europe expressed in standard deviations relative to the 1940–2000 period. **c** As in (a) but for 2023. **d** As in (b) but for 2023. **e** *Historical Context:* Reconstruction of MJJAS temperature anomalies⁴. Solid orange line represents the tree-ring based reconstruction. Solid gray line represents the uncertainty of the reconstruction. Solid brown line represents the 11-year running mean. Solid green line represents data from the E-OBS. Solid golden line represents data from Berkeley Earth Observatory. Solid blue line represents the multi-model-mean from EURO-CORDEX. The collected trees from the Pyrenees show a strong correlation ($r = 0.76$; $p \leq 0.001$; 1940–2020 CE) with instrumental MJJAS maximum temperatures. Despite being localized in the Pyrenees, the white box delineates areas where the reconstruction exhibits significant Pearson correlations ($p < 0.01$) with correlations

exceeding 0.6, indicating robust validation for WM countries⁴. The white circle marks the specific site of the temperature reconstruction. Extending this to 2022 (red circle) and 2023 (black circle) reaffirmed both as the peaks of 902 years of reconstructed data, marking the period since 2003 as the warmest since the Medieval era. The reconstruction’s ability to capture a wide range of climate variability is further highlighted by the yellow shading, which marks periods of solar minima (sunspots) associated with cooling anomalies. Additionally, the figure identifies 20 significant tropical volcanic eruptions, larger than the 1991 Pinatubo event, that coincide with these noted cooling periods. Thus, this reconstruction effectively documents diverse climate fluctuations, from the high-frequency cooling effects triggered by volcanic activity to the more gradual changes caused by variations in solar activity or the anthropogenic warming since the end of the 19th century. The historical multi-model mean is based on EURO-CORDEX evaluation runs, while future projections from EURO-CORDEX are presented for various RCPs scenarios based on different models (see supplementary Table S2).

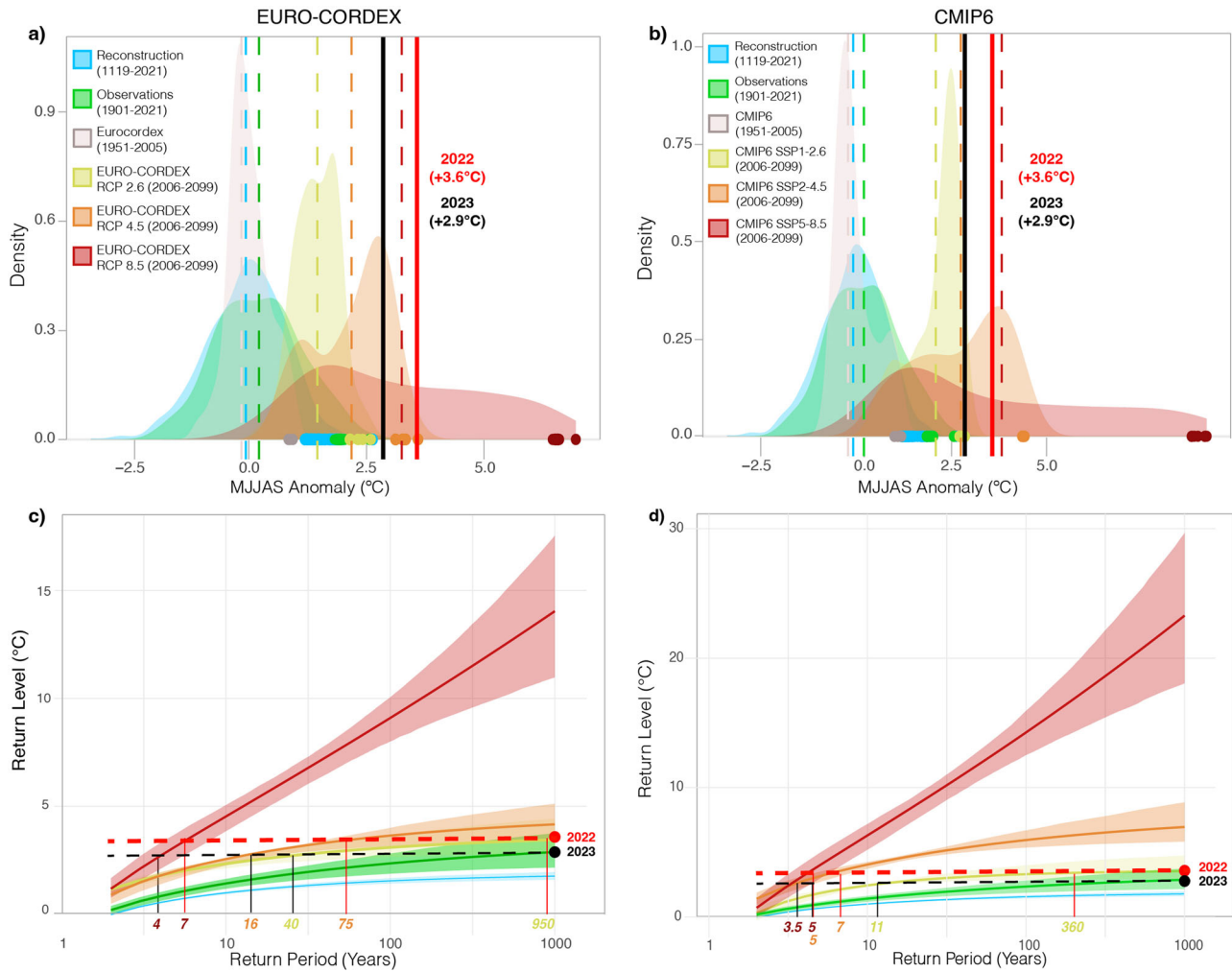


Fig. 2 | Maximum temperature anomaly distribution and return periods in the Western Mediterranean: Insights from reconstructions, observations, and future scenarios. **a** Comparative Climate Anomaly Analysis: Probability density functions illustrating Western Mediterranean climate anomalies, as inferred from tree-ring reconstructions, observational records (Berkeley Earth), and the average projections across three future climate scenarios for 1951–2005. Additionally, anomaly distributions against varying emission pathways are shown, showcasing the potential divergence in climate trajectories contingent on current policy decisions. Dashed lines represent the distributions’ means, while solid circles highlight the occurrence

of warm extremes, identified at the 95th percentile. Note that while the E-OBS dataset records a 2022 temperature anomaly of 3.9 °C, we have chosen to use the most conservative estimate in our analysis. **b** As in (a) but for CMIP6. **c** Frequency Projections for the 2022 and 2023 Extreme Warm Anomalies: This panel quantifies the recurrence interval (in years) of the exceptional warmth observed in 2022 (red vertical line) and 2023 (black vertical line), comparing estimates from a historical reconstruction, present-day observations, and projections within future climate scenarios. **d** as in (c) but for CMIP6.

For instance, future projections up to 2099 vary: under the mild RCP2.6 scenario, temperatures could rise by 1.67 °C; the RCP4.5 scenario projects a 2.26 °C increase; and the RCP8.5 scenario estimates a stark rise to an average of 4.35 °C, with extremes potentially surpassing 6 °C. Temperature projections under CMIP6 scenarios indicate higher values compared to EURO-CORDEX, with the extreme temperatures of 2023 aligning with the mean of SSP2-4.5 projections, and those of 2022 approaching but not reaching the mean of SSP5-8.5 projections. These estimates indicate that without significant mitigation efforts, future extremes are likely to surpass the record temperatures experienced in both 2022 and 2023.

The return periods of the 2022 and 2023 extremes, detailed in Fig. 2c, d, and Table S1, demonstrate that pre-2022 millennial reconstruction assigns a likelihood of less than once in 10,000 years (blue line, Fig. 2c) for such events, suggesting a minimal natural occurrence without anthropogenic influence. Instrumental data from 1901 to 2021, however, indicates and increased frequency, albeit still rare, with a maximum return period of once in 1000 years, and 2023 events slightly more frequent. Under future climate projections, the frequency of these extremes escalates: about once in 950 years for 2022 and in 40 years for 2023 under RCP2.6; once in 75 years for

2022 and 16 years for 2023 under the middle-of-the-road RCP4.5; and as often as once in 7 years for 2022 and once in 4 years for 2023 under RCP8.5, aligning such extremes with higher forcing scenarios (Fig. 2c). Comparative analysis of EURO-CORDEX and CMIP6 suggests more frequent occurrences under comparable scenarios, projecting the 2022-type extreme as a once every 7 years even under SSP2-4.5 (Fig. 2d). Although CMIP6 models show similar performance to CMIP5 models in projecting climate extremes¹⁶, CMIP6 ensemble projects amplified warming in the Mediterranean^{17,18}. This discrepancy highlights considerable uncertainties in future risk assessments, particularly given the premature manifestation of 2022’s conditions, initially projected to occur decades later. This situation warrants further research and necessitates modeling experiments that include regional climate models with CMIP6 to improve projection accuracy and thus inform to develop more robust adaptation strategies.

What are the potential causes of such extremes?

In 2023, the globe experienced the warmest temperatures on record since 1850¹⁹, driven not only by climate change but also by the Atlantic Multi-decadal Oscillation and a strong El Niño that began in June 2023²⁰. Warm

season temperatures over WM were exceptionally high, although lower than the record extremes of 2022. These years had contrasting Pacific conditions: El Niño-like in 2023 and La Niña-like in 2022 (Fig. 1a, c), yet neither significantly influence temperatures in the WM, highlighting a poor correlation with ENSO ($r = 0.14$, improving to 0.20, for warm anomalies above 1 °C). Additionally, the hypothesis that a circumglobal teleconnection pattern, influenced by subtropical heating and a positive phase of the Indian Ocean Dipole (IOD)²¹, contributed to these extremes is contradicted by the negative phase of the IOD during the same period of 2022, and the neutral phase present in 2023. This underscores the potential greater influence of Mediterranean and Atlantic SSTs on regional climate, with correlations since 1981 exceeding 0.8 ($n = 41$, $p < 0.01$) between land WM and adjacent Mediterranean SSTs. This link accounts for over 60% of the variance in regional land temperatures during the warm season, highlighting the importance of these factors in forecasting and developing adaptation strategies. Recent extremes, deviating significantly from observational data, align more with scenario simulations, underscoring climate change's role. Historical events such as the 2018 European heatwaves²² and the severe 2003 and 2018²³ droughts further corroborate this impact.

Overall, the extreme conditions in 2022 and 2023 were likely due to a combination of factors: precipitation deficits resulting in exceptionally dry soils, the prevalence of persistent high-pressure systems, and unusually warm SSTs in the Atlantic and Mediterranean. These thermal anomalies in the Mediterranean are particularly significant²⁴, as they not only contribute to the increased frequency and intensity of regional heatwaves²⁵, but acts as a catalyst for altering the hydrological dynamics, potentially enhancing summer precipitation extremes in adjacent areas^{26,27}. The influence of WM SSTs on regional extremes emphasizes the need for improved, high-resolution ocean modeling to better understand their impact on climate resilience amidst global changes.

Are Mediterranean countries prepared for the intensifying climate extremes?

Our analysis of the 2022 and 2023 summer heatwaves reveals a troubling truth: extreme climate events are not only becoming more common and intense²⁸, but are also occurring earlier than models have previously predicted. This trend is likely influenced by rising Mediterranean Sea surface temperatures, that have increased twice as fast as global averages²⁴. The exceptional intensity of the heat experienced during 2022 and continuing into 2023, likely unprecedented over the last millennium, is a clear indicator of the profound impact of current climate change. In fact, our integrated approach, combining instrumental records, proxy data, and climate model projections, suggests that such extremes would have been highly improbable in a pre-industrial climate. Criticism of how conceivable “business-as-usual” scenarios are, which often ignore mitigation efforts²⁹, is increasing. Instead, “middle-of-the-road” scenarios, which account for some level of intervention, are now considered more realistic³⁰. However, these scenarios, once thought to reflect conditions originally projected for 30–50 years in the future, correspond closely with the extremes observed in 2022 and 2023, emphasizing the immediate and pressing nature of what were once considered distant climate extremes.

The socioeconomic structure of Mediterranean countries, heavily dependent on tourism³¹ and agriculture, are becoming increasingly vulnerable due to more unpredictable and severe climate conditions. The consecutive 2022–23 heatwaves featured major challenges in WM nations like Italy and Spain, where summer tourism is crucial to the economy (~12–13% of GDP)³². Thus, rising temperatures raise concerns about the sustainability of these areas as tourist destinations and their economic future³¹. Nonetheless, such extreme weather events also produce environmental stresses with long-lasting effects on biodiversity³³, ecosystem services³⁴, and water resources³⁵, potentially leading to long-term ecological and societal degradation³⁶.

Given these challenges, it is imperative for policymakers to recognize and address both the increasing risk of extreme temperatures, and the more frequent and intense drought conditions driven by higher

evapotranspiration rates²³. Proactive planning and the implementation of adaptive measures are crucial to mitigate the potential disruptions to both the ecological systems and the economic structures dependent on them in these vulnerable regions. Such comprehensive approach will help sustain the natural environment and the economies that are intricately linked to it in the WM.

Methods

Instrumental land and marine temperature data

To evaluate the rarity of the warm seasons (May to September) in 2022 and 2023, we utilized instrumental datasets from the Berkeley Earth Observatory³⁷ (spatial resolution of 1°) and the European Observatory Dataset³⁸ (spatial resolution of 0.5°), which also contributed to the development of the Pyrenees tree-ring reconstruction⁴. We computed the mean for the geographic area from latitude 41 to 43°N and longitude –1 to 1.5°E. Our analysis focused on the temperature signal during the warm season, which demonstrated a strong spatial correlation across the WM countries⁴. Several tests were conducted (not shown) using an expanded geographic box over land; however, the findings on variability and trends were consistent with our initial results, thus we kept the original box. This methodological choice ensures consistency across the datasets used and provides a reliable basis for our conclusions regarding the extreme character of 2022 and 2023 warm seasons. Finally, to display a better representation of the events, and at the same time present a different product (reanalysis, instead of instrumental only) we used the ERA5 dataset³⁹ (Fig. 1a–d).

Sea surface temperatures

We analyzed satellite-derived sea surface temperature (SST) data⁴⁰ from 1981 to 2023 for the WM. To refine the data, we converted daily temperature readings into monthly averages. To mitigate potential biases from autocorrelation and underlying trends, we employed residuals from a linear regression model applied to the SST series, alongside comparable instrumental data (Berkeley Earth and E-OBS) and dendrochronological reconstructions. Our analysis reveals a robust correlation between land temperatures in the WM and adjacent sea surface temperatures since 1981. Satellite observations show strong associations with both instrumental records and tree-ring data ($r = 0.80$, $n = 41$, $p < 0.01$; $r = 0.77$, $n = 41$, $p < 0.01$, respectively). This correlation intensifies for extreme temperature events, where land temperature anomalies surpass the 80th percentile ($r = 0.85$, $n = 9$, $p < 0.01$; $r = 0.78$, $n = 9$, $p < 0.01$, respectively), underscoring a significant link between regional terrestrial and marine thermodynamics.

Tree-ring reconstruction

The high-resolution, absolute dated reconstruction is composed of maximum latewood density (MXD) samples from 534 living and relic *Pinus uncinata* trees at the upper treeline ecotones in the Spanish central Pyrenees (Parque Nacional de Aigüestortes y Estany de Sant Maurici), covering the period from 1119 to 2020 CE⁴. This new MXD composite chronology shows a strong correlation with the May–September mean temperatures over the WM region ($r = 0.76$; $p \leq 0.001$; 1950–2020 CE). The reconstruction is an updated product from previous efforts^{41,42}, including improved replication of earlier periods and the use of a new detrending approach to better retain high-to-low frequency variability domains. The ensemble-based reconstruction indicates an unprecedented increase in summer temperatures since 2003 CE. Based on the strong and consistent correlation we estimated the warm seasons of 2021, 2022, and 2023 in the reconstruction through linear regression.

Climate model simulations

We employed both EURO-CORDEX¹² (see supplementary Table S2 for selected simulations) and CMIP6¹⁴ (see supplementary Table S3) climate projections to assess regional climate variability and extremes. We primarily showcased results from EURO-CORDEX's 0.44° resolution models, over the same coordinates used for the instrumental period, due to its enhanced spatial resolution, the model offers a finer representation of regional climate

phenomena across WM countries. As with the instrumental data, numerous tests were conducted using an expanded geographic box over land. However, since the findings on variability and trends aligned with our initial results, we retained the original box. This finer resolution is crucial for capturing detailed regional phenomena and aligning with observed climate trends, making EURO-CORDEX models particularly suited for localized impact assessments¹². However, it is important to recognize that higher resolution does not always result in improved accuracy in all aspects of climate modeling⁴³. Note also that EURO-CORDEX downscaling relies on regional models with GCM CMIP5 SSTs as boundary conditions without a regional ocean model.

While CMIP6 models contribute with global insights, their coarser resolution renders them less effective for detailed regional analysis⁴⁴. Nevertheless, the spatial dimension of the anomalies discussed herein is well captured by the CMIP6 resolution. Therefore, including the high-resolution data from EURO-CORDEX alongside the updated external forcings in CMIP6 reinforces our analysis by utilizing the strengths of both model ensembles independently. Our methodology included calculating the multimodel median to mitigate model-specific biases while preserving internal variability. This strategy effectively captures temperature extremes⁴⁵. Finally, we determined uncertainty boundaries using the 10th and 90th percentiles from each model.

Analysis

To calculate the probability density functions (PDFs), we analyzed data across several temporal and scenario-based contexts. We utilized millennium-length tree-ring reconstructions for historical context, instrumental data from the Berkeley Earth Observatory for current climate assessments, and the multimodel mean from EURO-CORDEX for the period 1951–2005. For future projections, PDFs were generated for three different scenarios: RCP2.6, RCP4.5, and RCP8.5, spanning from 2006 to 2099. The analysis was also performed using CMIP6 projections.

We employed the *ismev* package⁴⁶ with R^{47} to fit Generalized Extreme Value distributions⁴⁸, which have been used for modeling temperature extremes in millennial context⁴⁹ and are particularly useful for risk assessment⁵⁰. We opted for L-moments to estimate parameters due to their robustness against outliers and effectiveness with the small sample sizes typical of extreme event datasets⁵¹. L-moments are advantageous for their reduced bias in skewed distributions and simplify the computational process compared to iterative methods like maximum likelihood estimations. The cumulative distribution function of the GEV distribution is given by:

$$G(z) = \exp\left(-\left[1 + \xi \frac{(z - \mu)}{\sigma}\right]^{-1/\xi}\right)$$

where: μ determines the center of the distribution, σ and ξ determine the scale and shape of the distribution respectively, while z is the maximum temperature mean of MJJAS. For the GEV, the block maxima method is typically used, where z represents the maximum (or minimum) value observed in each period/block (e.g., year). Thus, the return level calculation (z_T), associated with a specific return period T (1000 years, because it is roughly the tree-ring reconstruction length) is formulated as:

$$Z_T = \mu - \frac{\sigma}{\xi} \left(\left[-\log\left(1 - \frac{1}{T}\right) \right]^{-\xi} - 1 \right)$$

Additionally, to further assess the uncertainty of our findings and establish the upper and lower extremes, we performed a bootstrap analysis with 1000 iterations, enhancing the reliability of our results and providing a comprehensive evaluation of the variability in climatic extremes essential for analyzing temperature anomalies historically. To calculate return periods, we used the more conservative 3.6 °C anomaly reported by Berkeley Earth

over the 3.9 °C from the E-OBS dataset for 2022, and 2.9 °C from the E-OBS for 2023 (2.86 °C Berkeley).

Data availability

The reconstruction data are available upon request to ub223@cam.ac.uk. ERA5 data is publicly available from <https://doi.org/10.24381/cds.143582cf>, E-OBS from <https://www.ecad.eu/download/ensembles/download.php>, CMIP6 data are accessible through <https://wcrp-cmip.org/cmip-data-access/>, and CORDEX simulations through <https://cordex.org/data-access/esgf/>.

Code availability

All code for data analysis and figure replication can be requested to: Ernesto.tejedor@mncn.csic.es.

Received: 23 May 2024; Accepted: 11 September 2024;

Published online: 18 September 2024

References

1. MedECC. *Climate and Environmental Change in the Mediterranean Basin—Current Situation and Risks for the Future*. First Mediterranean Assessment Report [Cramer, W., Guiot, J., Marini, K. (eds.)] 632pp, ISBN 978-2-9577416-0-1, (Union for the Mediterranean, Plan Bleu, UNEP/MAP, 2020).
2. Ali, E., et al. Cross-Chapter Paper 4: Mediterranean region. In: *Climate Change 2022: Impacts, Adaptation and Vulnerability*. Contribution of Working Group II to the Sixth Assessment Report of the Intergovernmental Panel on Climate Change [H.-O. Pörtner, D. C. Roberts, M. Tignor, E. S. Poloczanska, K. Mintenbeck, A. Alegría, M. Craig, S. Langsdorf, S. Lösschke, V. Möller, A. Okem, B. Rama (eds.)] pp. 2233–2272, (Cambridge University Press, 2022).
3. Serrano-Notivol, R. et al. Unprecedented warmth: a look at Spain's exceptional summer of 2022. *Atmos. Res.* **293**, 106931 (2023).
4. Büntgen, U. et al. Recent summer warming over the western Mediterranean region is unprecedented since medieval times. *Glob. Planet. Chang.* **232**, 104336 (2024).
5. Copernicus Climate Change Service (C3S) *European State of the Climate*, Full report: climate.copernicus.eu/ESOTC/2022 (2023).
6. Esper, J., Torbenson, M. & Büntgen, U. 2023 summer warmth unparalleled over the past 2000 years. *Nature* **631**, 94–97 (2024).
7. Vidaller, I. et al. The Aneto glacier's (Central Pyrenees) evolution from 1981 to 2022: ice loss observed from historic aerial image photogrammetry and remote sensing techniques. *Cryosphere* **17**, 3177–3192 (2023).
8. Cancer-Pomar, L., Fernández-Jarne, G., Cuchi, J. A. & del Valle-Melendo, J. The *Infierno* Glacier (Pyrenees, Aragon, Spain): evolution 2016–2022. *Geosciences* **13**, 40 (2023).
9. van der Woude, A. et al. Temperature extremes of 2022 reduced carbon uptake by forests in Europe. *Nat. Commun.* **14**, 6218 (2023).
10. Ballester, J. et al. Heat-related mortality in Europe during the summer of 2022. *Nat. Med.* **29**, 1857–1866 (2023).
11. Copernicus Climate Change Service (C3S), 2024: European State of the Climate, Summary. <https://doi.org/10.24381/bs9v-8c66> (2023).
12. Jacob, D. et al. Regional climate downscaling over Europe: perspectives from the EURO-CORDEX community. *Reg. Environ. Chang.* **20**, 51 (2020).
13. Moss, R., Edmonds, J. & Hibbard, K. et al. The next generation of scenarios for climate change research and assessment. *Nature* **463**, 747–756 (2010).
14. Eyring, V. et al. Overview of the Coupled Model Intercomparison Project Phase 6 (CMIP6) experimental design and organization. *Geosci. Model Dev.* **9**, 1937–1958 (2016).
15. Riahi, K. et al. The Shared Socioeconomic Pathways and their energy, land use, and greenhouse gas emissions implications: an overview. *Glob. Environ. Change* **42**, 153–168 (2017).

16. Coppola, E. et al. Assessment of the European Climate Projections as simulated by the large EURO-CORDEX regional and global climate model ensemble. *J. Geophys. Res. Atmos.* **126**, e2019JD032356 (2021).
17. Kim, Y.-H., Min, S.-K., Zhang, X., Sillmann, J. & Sandstad, M. Evaluation of the CMIP6 multi-model ensemble for climate extreme indices. *Weather Clim. Extremes* **29**, 100269 (2020).
18. Cos, J. et al. The Mediterranean climate change hotspot in the CMIP5 and CMIP6 projections. *Earth Syst. Dyn.* **13**, 321–340 (2022).
19. NOAA National Centers for Environmental Information, *Monthly Global Climate Report for Annual 2023*, published online January 2024, retrieved on 11 April 2024 from <https://www.ncei.noaa.gov/access/monitoring/monthly-report/global/202313> (2023).
20. Li, K., Zheng, F., Zhu, J., & Zeng, Q.-C. El Niño and the AMO sparked the astonishingly large margin of warming in the global mean surface temperature in 2023. *Adv. Atmos. Sci.* <https://doi.org/10.1007/s00376-023-3371-4> (2024).
21. Behera, S., Ratnam, J. V., Masumoto, Y. & Yamagata, T. Origin of extreme summers in Europe: the Indo-Pacific connection. *Clim. Dyn.* **41**, 663–676 (2013).
22. Rousi, E., Kornhuber, K., Beobide-Arsuaga, G., Luo, F. & Coumou, D. Accelerated western European heatwave trends linked to more-persistent double jets over Eurasia. *Nat. Commun.* **13**, 3851 (2022).
23. Treydte, K. et al. Recent human-induced atmospheric drying across Europe unprecedented in the last 400 years. *Nat. Geosci.* **17**, 58–65 (2024).
24. Urdiales-Flores, D., Zittis, G. & Hadjinicolaou, P. et al. Drivers of accelerated warming in Mediterranean climate-type regions. *npj Clim. Atmos. Sci.* **6**, 97 (2023).
25. Pastor, F. & Khodayar, S. Marine heat waves: characterizing a major climate impact in the Mediterranean. *Sci. Total Environ.* **861**, 160621 (2023).
26. Drobinski, P., Silva, N. D. & Panthou, G. et al. Scaling precipitation extremes with temperature in the Mediterranean: past climate assessment and projection in anthropogenic scenarios. *Clim. Dyn.* **51**, 1237–1257 (2018).
27. Volosciuk, C., Maraun, D. & Semenov, V. et al. Rising mediterranean sea surface temperatures amplify extreme summer precipitation in Central Europe. *Sci. Rep.* **6**, 32450 (2016).
28. IPCC: *Climate Change 2021: The Physical Science Basis. Contribution of Working Group I to the Sixth Assessment Report of the Intergovernmental Panel on Climate Change* [Masson-Delmotte, V., P. Zhai, A. Pirani, S. L. Connors, C. Péan, S. Berger, N. Caud, Y. Chen, L. Goldfarb, M. I. Gomis, M. Huang, K. Leitzell, E. Lonnoy, J. B. R. Matthews, T. K. Maycock, T. Waterfield, O. Yelekçi, R. Yu, and B. Zhou (eds.)]. <https://doi.org/10.1017/9781009157896> (Cambridge University Press, 2024) (In press).
29. Hausfather, Z. & Peters, G. P. Emissions - the 'business as usual' story is misleading. *Nature* **577**, 618–620 (2020).
30. Pedersen, J. S. T. et al. Variability in historical emissions trends suggests a need for a wide range of global scenarios and regional analyses. *Commun. Earth Environ.* **1**, 41 (2020).
31. Matei, N., et al. *Regional Impact of Climate Change on European Tourism Demand*, EUR 31519 EN, ISBN 978-92-68-03925-0, <https://doi.org/10.2760/899611>, JRC Technical Report 131508 (Publications Office of the European Union, 2023).
32. Ramaciotti, C. *The Turbulent Connection: the impact of climate change on travellers' demand*/New Atlas of Destinations and Seasonality. Mabrian. 2021. Last accessed March. <https://mabrian.com/blog/the-consequences-for-tourism-of-climate-change-in-the-mediterranean/> (2024).
33. Habibullah, M. S., Din, B. H., Tan, S.-H. & Zahid, H. Impact of climate change on biodiversity loss: global evidence. *Environ. Sci. Pollut. Res.* **29**, 1073–1086 (2022).
34. Kubiszewski, I., Costanza, R., Anderson, S., & Sutton, P. *Environmental Assessments*. <https://doi.org/10.4337/9781788976879.00016> (Edward Elgar Publishing, 2020).
35. Gudmundsson, L. et al. Globally observed trends in mean and extreme river flow attributed to climate change. *Science* **371**, 1159–1162 (2021).
36. Menzel, A. et al. Climate change fingerprints in recent European plant phenology. *Glob. Change Biol.* **26**, 2599–2612 (2020).
37. Rohde, R. A. & Hausfather, Z. The Berkeley Earth Land/Ocean Temperature Record. *Earth Syst. Sci. Data* **12**, 3469–3479 (2020).
38. Cornes, R. C., van der Schrier, G., van den Besselaar, E. J. M. & Jones, P. D. An ensemble version of the E-OBS temperature and precipitation data sets. *J. Geophys. Res. Atmos.* **123**, 9391–9409 (2018).
39. Bell, B. et al. The ERA5 global reanalysis: preliminary extension to 1950. *Q. J. R. Meteorol. Soc.* **147**, 4186–4227 (2021).
40. Merchant, C. et al. Satellite-based time-series of sea-surface temperature since 1981 for climate applications. *Sci. Data* **6**, 1–18 (2019).
41. Büntgen, U., Frank, D., Grudd, H. & Esper, J. Long-term summer temperature variations in the Pyrenees. *Clim. Dyn.* **31**, 615–631 (2008).
42. Büntgen, U. et al. New tree-ring evidence from the Pyrenees reveals Western Mediterranean climate variability since medieval times. *J. Clim.* **30**, 5295–5318 (2017).
43. Giorgi, F., Raffaele, F. & Coppola, E. The response of precipitation characteristics to global warming from climate projections. *Earth Syst. Dyn.* **10**, 73–89 (2019).
44. Soares, P. M. M., Johannsen, F., Lima, D. C. A., Lemos, G., Bento, V. A. & Bushenkova, A. High-resolution downscaling of CMIP6 Earth system and global climate models using deep learning for Iberia. *Geosci. Model Dev.* **17**, 229–259 (2024).
45. Li, C., Zwiers, F., Zhang, X., Li, G., Sun, Y. & Wehner, M. Changes in annual extremes of daily temperature and precipitation in CMIP6 models. *J. Clim.* **34**, 3441–3460 (2021).
46. Stephenson. *RdpbAG. _ismev: An Introduction to Statistical Modeling of Extreme Values. R package version 1.42*, <https://CRAN.R-project.org/package=ismev> (2018).
47. R Core Team. *R: A Language and Environment for Statistical Computing*. <https://www.R-project.org/> (R Foundation for Statistical Computing, 2024).
48. Coles, S. *An Introduction to Statistical Modeling of Extreme Values* (Springer, 2001).
49. Huang, W. K., Stein, M. L., McInerney, D. J., Sun, S. & Moyer, E. J. Estimating changes in temperature extremes from millennial-scale climate simulations using generalized extreme value (GEV) distributions. *Adv. Stat. Clim. Meteorol. Oceanogr.* **2**, 79–103 (2016).
50. Rypkema, D., & Tuljapurkar, S. Modeling extreme climatic events using the generalized extreme value (GEV) distribution. In A. S. R. Srinivasa Rao & C. R. Rao (Eds.), *Handbook of Statistics* (Vol. 44, pp. 39–71) (Elsevier, 2021).
51. Hossain, I., Imteaz, M. A. & Khastagir, A. Effects of estimation techniques on generalised extreme value distribution (GEVD) parameters and their spatio-temporal variations. *Stoch. Environ. Res. Risk Assess.* **35**, 2303–2312 (2021).

Acknowledgements

E.T. received funding from a European Union Marie Skłodowska-Curie Action (ITHACA-101024389), and the Comunidad de Madrid program Atracción Talento “César Nombela” grant number 2023-T1/ECO-29118. R.S.N. is supported by grant RYC2021-034330-I funded by MCIN/AEI/10.13039/501100011033 and by “European Union NextGenerationEU/PRTR”. J.F.G.R. is supported by project PID2021-126696OB-C21 of the MCIN. J.E. and U.B. are supported by the ERC Advanced projects MONOSTAR (AdG 882727), the ERC Synergy project SYNERGY-PLAGUE (101118880), the Czech Science Foundation grant HYDRO8 (23-08049S), the co-funded EU project AdAgriF (CZ.02.01.01/00/22_008/0004635), and the Centre for Interdisciplinary Research (ZIF) in Bielefeld, Germany.

Author contributions

E.T. designed and conceived the study, with further enhancements contributed by G.B., R.S.N., J.F.G.R., U.B., and J.E. U.B. and J.E. supplied the tree-ring data. E.T. conducted the data analysis and drafted the initial version of the manuscript. All authors contributed to the revisions and approved the final manuscript.

Competing interests

The authors declare no competing interests.

Additional information

Supplementary information The online version contains supplementary material available at <https://doi.org/10.1038/s41612-024-00771-6>.

Correspondence and requests for materials should be addressed to Ernesto Tejedor.

Reprints and permissions information is available at <http://www.nature.com/reprints>

Publisher's note Springer Nature remains neutral with regard to jurisdictional claims in published maps and institutional affiliations.

Open Access This article is licensed under a Creative Commons Attribution-NonCommercial-NoDerivatives 4.0 International License, which permits any non-commercial use, sharing, distribution and reproduction in any medium or format, as long as you give appropriate credit to the original author(s) and the source, provide a link to the Creative Commons licence, and indicate if you modified the licensed material. You do not have permission under this licence to share adapted material derived from this article or parts of it. The images or other third party material in this article are included in the article's Creative Commons licence, unless indicated otherwise in a credit line to the material. If material is not included in the article's Creative Commons licence and your intended use is not permitted by statutory regulation or exceeds the permitted use, you will need to obtain permission directly from the copyright holder. To view a copy of this licence, visit <http://creativecommons.org/licenses/by-nc-nd/4.0/>.

© The Author(s) 2024